Eighth Hungarian Conference on Computer Graphics and Geometry, Budapest, 2016

Multi-sided Surfaces with Fullness Control

Péter Salvi[1,2], Tamás Várady[1]

[1] Budapest University of Technology and Economics, Hungary
[2] Shizuoka University, Japan

Abstract

Multi-sided surfaces are important in several areas of Computer-Aided Geometric Design, including curve network based design, approximation of triangular meshes, hole filling, and so on. In the majority of surface representations, the boundary constraints entirely determine the interior of these patches, however, frequently there is a need to have additional design freedom for shaping the surface. In this paper, we investigate new multi-sided surfaces, where such interior control is possible. As a reference, we take a recent variant of the Gregory patch,[8] and compare it with two new representations: (i) a transfinite patch defined by boundary ribbons (curves and cross-derivatives) and a single surface point to set in the middle, and (ii) a recently published, new n-sided Bézier patch,[10] defined by a grid of control points. We will discuss the different degrees of freedom for shape adjustment, and illustrate our results by a few examples showing mesh approximation quality.

1. Introduction

The majority of free-form models in Computer Aided Geometric Design is almost exclusively represented by quadrilateral surfaces, however there is a definite demand in the CAD industry for using multi-sided patches within structures of general topology (arbitrary number of sides, arbitrary vertex valency, T-nodes, etc.). There are several well-known approaches to overcome this problem, such as surface trimming, internal splitting into quadrilateral patches, or subdivision. Our current interest is to investigate genuine n-sided patches, where artificial intricacies coming from the tensor product schemes are avoided and natural structures can be created for shape design and/or reproduction. Here we will deal with two different approaches used for multi-sided patches: transfinite surfaces and control point based patches.

The main advantage of transfinite surfaces is that they are fundamentally determined by their boundaries, and these boundaries may be represented by parametric curves of any form. In most cases, the patches are defined not only by positional constraints, but also by *ribbon* surfaces—interpolants that carry cross-derivative constraints. This facilitates the smooth connection of adjacent patches. In the majority of transfinite schemes, the interpolation of the ribbons determines the entire patch, and there is only a limited control to modify the interior by means of setting the magnitude of cross-derivatives. The default patch, or even the optimized shape may not be sufficiently good, and further fullness control is often required for free-form design or shape approximation. In Section 4 we will look at a conventional transfinite representation, the *corner-based* (CB) patch, a variant of Gregory's scheme, as was proposed by Salvi et al.[8] In Section 5 we introduce a new transfinite representation, the *midpoint* (MP) patch, where in addition to the ribbons, the middle point of the surface can also be edited. The advantages of this surface formulation will be shown and its interpolation property will also be proven.

Control point based multi-sided patches are defined by a special grid structure. The boundaries must be defined by standard control point based curves, such as Bézier or B-spline curves, and the cross-derivatives are determined by the first two rows of control points of the multi-sided grid. In this case we have a somewhat reversed situation, as we can have a sufficiently large number of control points over the interior, however, it is far from obvious how to adjust the interior control points when the boundaries are modified. A recently published, novel n-sided patch,[10] that generalizes quadrilateral Bézier surfaces, overcomes this problem. Interior control points can be edited when needed, or derived automatically from the boundary control points, as well, using a special degree elevation/reduction algorithm. An additional center control point is available for adjusting the middle point of the patch (see Section 6).

In Section 7, we compare the above representations through shape approximation examples.

2. Previous Work

There is an extensive research on transfinite surface interpolation, see e.g. our review paper.[9] More recent developments include the generalized Coons patch[8] and an extension of the Gregory patch with G^2-continuous boundaries.[7] The representation introduced in this paper is based on the *corner-based* (CB) Gregory patch in Salvi et al.[8]

Várady et al.[11] presents another transfinite construction that has control over the interior of the surface. It is based on a patch originally proposed by Kato,[5] and referred to as *side-based* (SB) patch in Salvi et al.[8] Its blending functions are extended to incorporate a new middle surface interpolant. This can also be applied to CB patches. The blending functions we are going to introduce here have different properties, see details in Section 5.

There are several control network based multi-sided patch formulations. Hosaka and Kimura[4] published quadratic and cubic n-patches, which were later extended to boundaries of arbitrary degrees by Zheng and Ball.[12, 1] These, however, use high-degree expressions, and are limited to 3–6 sides.

Another early result is the S-patch,[6] which generalizes Bézier surfaces to n sides, using multinomials and a convex polygonal domain. Unfortunately, its manual modification is quite difficult, due to the high number of control points and their complex topology.

In a recent paper, we have presented a different multi-sided generalization of the Bézier surface,[10] and an algorithm that merges Bézier patches of different degrees into a single multi-sided surface in a natural way. This patch representation will be reviewed in Section 6.

3. Transfinite Surface Interpolation

In the following two sections, we will describe two transfinite surface representations. Since the midpoint patch is a modification of the corner-based patch, the two are very similar. This section reviews the basic construction of these surfaces along the lines of Salvi et al.[7]

Both patches are defined over an n-sided regular polygon in the (u,v) plane, interpolating linear *ribbon surfaces* associated with the sides of the polygon. For each side Γ_i, we define local parameters $s_i = s_i(u,v)$ and $h_i = h_i(u,v)$. The *side parameter* s_i varies linearly on Γ_i between 0 and 1, while the *distance parameter* h_i vanishes on Γ_i and increases monotonically within the domain, as we move away from Γ_i. The ribbons are defined as

$$R_i(s_i,h_i) = P_i(s_i) + w_i h_i T_i(s_i), \tag{1}$$

where $P_i(s_i)$ defines the i-th boundary curve, $T_i(s_i)$ is the related cross-derivative, and w_i denotes a scalar multiplier that controls the magnitude of the ribbon.

Both schemes are based on *corner interpolant* surfaces $I_{i,i-1}$, that interpolate the $(i-1)$-th and i-th ribbons both positionally and in a derivative sense. (Sides are indexed cyclically, with 1 coming after n.) Using the local side parameters

$$\begin{aligned} I_{i,i-1}(u,v) \;=\; & R_{i-1}(s_{i-1},s_i) + R_i(s_i,1-s_{i-1}) - \\ & Q_{i,i-1}(s_i,s_{i-1}). \end{aligned} \tag{2}$$

The correction term $Q_{i,i-1}$ is needed to ensure the reproduction of the two ribbons at the boundary:

$$\begin{aligned} Q_{i,i-1}(s_i,s_{i-1}) \;=\; & P_i(0) + s_i T_{i-1}(1) + (1-s_{i-1}) T_i(0) + \\ & (1-s_{i-1}) s_i W_{i,i-1}, \end{aligned} \tag{3}$$

where $W_{i,i-1}$ denotes the mixed partial derivative at corner $(i-1,i)$. (We assume compatible twists, otherwise rational terms can be used.)

In the final surface equations the corner interpolants are multiplied by special blending functions, that maintain the interpolation properties and eliminate the contribution of the corner interpolants associated with other sides. The equation of the CB patch is given as

$$S_{\mathrm{CB}}(u,v) = \sum_{i=1}^{n} I_{i,i-1}(u,v) B_{i,i-1}(u,v), \tag{4}$$

while the equation of the MP patch is

$$S_{\mathrm{MP}}(u,v) = \sum_{i=1}^{n} I_{i,i-1}(u,v) B^{\mathrm{RH}}_{i,i-1}(u,v) + P_0 B^{\mathrm{RH}}_0(u,v). \tag{5}$$

Although the same sort of corner interpolants $I_{i,i-1}$ are used, these are multiplied by different blending functions ($B_{i,i-1}$ and $B^{\mathrm{RH}}_{i,i-1}$, respectively), and there is also an extra term for the midpoint patch. In the following sections we will discuss how the patches and blending functions are constructed, and explain why different surface characteristics are obtained.

4. The Corner-based (CB) Patch

The CB patch is an extended variant of the classical Gregory patch,[2] as was recently presented in the papers by Salvi et al.[8, 7] In order to make the CB patch definition complete, we need to parameterize the domain and define blending functions. We revisit the well-known *radial sweepline* method to determine the $s_i(u,v)$ and $h_i(u,v)$ parameters. Take a domain point (u,v), and connect it with a line to the intersection point of the extended polygon sides Γ_{i-1} and Γ_{i+1}. This line intersects Γ_i at point Q, and defines a ratio in $[0,1]$, that is equal to s_i, see Figure 1. The distance parameter h_i is generally defined as $\|(u,v)-Q\|$, however, other measures, such as the perpendicular distance to Γ_i can also be used.

The corner interpolants are determined by the side parameters; the blending functions are defined as a function

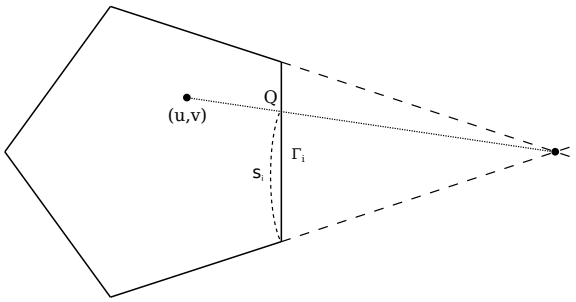

Figure 1: Construction of the radial parameterization.

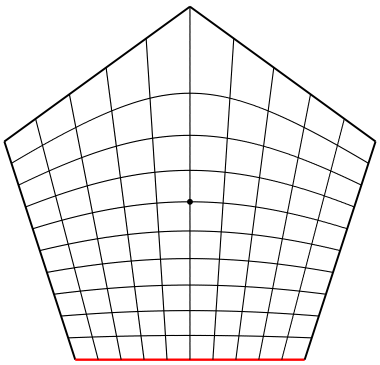

Figure 2: Constant parameter lines of the barycentric parameterization related to the red side, with resolution 1/10.

of the distance parameters $h_i(u,v)$. Introducing the notation $D_{i,i-1} = \prod_{k \notin \{i,i-1\}} h_k^2$, the blending functions are defined as

$$B_{i,i-1}(u,v) = \frac{D_{i,i-1}}{\sum_{j=1}^{n} D_{j,j-1}} = \frac{1/(h_i h_{i-1})^2}{\sum_{j=1}^{n} 1/(h_j h_{j-1})^2}. \quad (6)$$

Clearly $\sum_i B_{i,i-1}(u,v) = 1$ for each (u,v) point within the domain. These blending functions satisfy the basic requirement of smoothly eliminating the effect of the corner interpolants: $B_{i,i-1}$ is 1 at the corner $(i-1,i)$ and decreases to 0 as it reaches the adjacent corners $(i-2,i-1)$ and $(i,i+1)$; it is zero on the remaining sides Γ_j, $j \notin \{i-1,i\}$ with zero cross-derivatives. This construction guarantees the reproduction of the ribbons, as well, since $B_{i,i-1}(u,v) + B_{i+1,i}(u,v) = 1$ everywhere on side Γ_i, and it can be shown that the derivative constraints are also satisfied, see details in the original paper.

This completes the definition of the CB patch. Note, that the fullness of the patch can only be modified to a limited extent by the scalar multipliers w_i. In the following section we describe a scheme that provides an extra degree of freedom to shape the interior of the patch.

5. The Midpoint (MP) Patch

We are going to introduce an alternative blending function that allows for an extra control in the surface interior. In order to guarantee interpolation of the boundaries, we will first describe a parameterization based on barycentric coordinates.

5.1. Barycentric Parameterization

Generalized barycentric coordinates have been intensely investigated, see e.g. Hormann and Floater.[3] Having a polygon with vertices $V_1,..,V_n$, any point (u,v) in the interior can be expressed as a barycentric combination of the vertices, with the basic properties

$$\sum_{i=1}^{n} \lambda_i(u,v) V_i = (u,v), \quad \sum_{i=1}^{n} \lambda_i(u,v) = 1, \quad \lambda_i(V_j) = \delta_{ij}. \quad (7)$$

The elements of the n-tuple $\{\lambda_1,...,\lambda_n\}$ represent the barycentric coordinates. Using these, it is possible to define appropriate side and distance parameters for n-sided patches:

$$s_i = \lambda_i / (\lambda_{i-1} + \lambda_i), \qquad h_i = 1 - \lambda_{i-1} - \lambda_i. \quad (8)$$

It is easy to show, that the s_i parameters represent a family of sweeping lines within the domain, and the h_i parameters satisfy the basic distance properties (see Section 3). In addition, h_i increases linearly on Γ_{i-1} and Γ_{i+1}, and takes the value 1 along all "distant" sides, i.e., $h_i = 1$ for all points on the domain edges Γ_j, where $j \notin \{i-1,i,i+1\}$. Due to the linearity of the parameters on side Γ_i, the following equations also hold:

$$s_i = h_{i-1} \quad \text{and} \quad 1 - s_i = h_{i+1}. \quad (9)$$

This parametrization was suggested first in Várady et al.,[10] and it will be used for both the MP and GB patches in this paper. As an example, the isolines in a five-sided domain are shown in Figure 2.

5.2. Rational Hermite Blending Functions

As it was pointed out earlier, the midpoint patch is very similar to the CB patch, but it uses different corner blending functions (marked with RH), comprised of a rational expression with cubic Hermite polynomials:

$$B^{\mathrm{RH}}_{i,i-1}(u,v) = \frac{h_i H(1-s_{i-1}) H(h_{i-1}) + h_{i-1} H(s_i) H(h_i)}{h_i + h_{i-1}}, \quad (10)$$

where

$$H(x) = (1-x)^3 + 3(1-x)^2 x \quad (11)$$

with the following properties:

$$H(0) = 1, \qquad H(1) = 0, \quad (12)$$

$$H'(0) = 0, \qquad H'(1) = 0, \quad (13)$$

and also

$$H'(x) = H'(1-x). \tag{14}$$

These blending functions behave in the same manner as the distance-based blending functions of CB patches. Note, that although they are based on the relatively complex barycentric coordinates, the blend functions themselves have become much simpler. The denominator of RH blends is linear, and the numerator is only quartic w.r.t. the local parameters, independently of the number of sides. Compare this to the distance-based blend functions, where the rational degree grows with the number of sides.

Observe that these blending functions do not sum to 1; in other words they are *weight deficient*. In order to ensure convex combination and affine invariance, we introduce an additional, *central blending function* that compensates this weight deficiency:

$$B_0^{\mathrm{RH}}(u,v) = 1 - \sum_{i=1}^{n} B_{i,i-1}^{\mathrm{RH}}(u,v). \tag{15}$$

In this way it is possible to associate another surfacing term with $B_0^{\mathrm{RH}}(u,v)$ and gain additional design freedom for the interior. The value and the derivative of $B_0^{\mathrm{RH}}(u,v)$ vanish on all boundaries, thus the interior can be adjusted without violating the interpolation properties. We can choose an arbitrary middle point P_0, and then adding the term $P_0 B_0^{\mathrm{RH}}(u,v)$ completes the definition of the MP patch, as was given earlier in Eq. (5).

5.3. Setting the Central Control Point

We present two strategies for the placement of P_0; the same ideas were used in Várady et al.[10] As a default location, we can take the mass center of the "middle" points of the corner interpolants:

$$P_0 = \frac{1}{n} \sum_{i=1}^{n} I_{i,i-1}(0.5, 0.5). \tag{16}$$

As an alternative, the user can set a position C for the surface center, i.e., a point associated with the central point (u_0, v_0) of the domain polygon. Then we can compute P_0 by

$$P_0 = \frac{1}{B_0^{\mathrm{RH}}(u_0,v_0)} \left[C - \sum_{i=1}^{n} I_{i,i-1}(u_0,v_0) B_{i,i-1}^{\mathrm{RH}}(u_0,v_0) \right]. \tag{17}$$

The "strength" of the central control point depends on the number of sides. Table 1 shows $B_0^{\mathrm{RH}}(u_0,v_0) = 1 - \frac{n}{2} H(\frac{n-2}{n})$ for various values of n. Later we will discuss the modification of these values via reparameterization of the distance parameters (see Section 6.1).

	$n=5$	$n=6$	$n=7$	$n=8$
B_0^{RH}	$\frac{3}{25} = 0.12$	$\frac{2}{9} \approx 0.22$	$\frac{15}{49} \approx 0.31$	$\frac{3}{8} \approx 0.38$

Table 1: Blend deficiencies of the MP patch at the domain center as a function of the number of sides.

5.4. Proof of Interpolation

For a point (u,v) on Γ_i, we need to prove

$$S(u,v) = I_{i,i-1}(s_i, s_{i-1}) = I_{i+1,i}(s_{i+1}, s_i), \tag{18}$$

$$S'(u,v) = I_{i,i-1}(s_i, s_{i-1})' = I_{i+1,i}(s_{i+1}, s_i)', \tag{19}$$

where x' denotes a directional derivative by an arbitrary direction in the (u,v) plane.

Blends based on different sides vanish, i.e., $B_{j,j-1}^{\mathrm{RH}} = 0$, where $j \notin \{i, i+1\}$, as we have one of four situations: (i) $h_{j-1} = h_j = 1$, (ii) $h_{j-1} = 1$ and $s_j = 1$, (iii) $h_j = 1$ and $s_{j-1} = 0$, or (iv) $s_{j-1} = 0$ and $s_j = 1$. In all cases a Hermite polynomial becomes zero in both terms of the numerator. The same reasoning works also for the derivatives, due to Equation (13). Also, using Equations (9) and (14), straightforward algebra leads to

$$B_{i,i-1}^{\mathrm{RH}}(u,v)' = H'(s_i) s_i' = -B_{i+1,i}^{\mathrm{RH}}(u,v). \tag{20}$$

In other words, for a point on Γ_i, we have

$$S(u,v) = I_{i,i-1}(s_i, s_{i-1}) B_{i,i-1}^{\mathrm{RH}}(u,v) + I_{i+1,i}(s_{i+1}, s_i) B_{i+1,i}^{\mathrm{RH}}(u,v), \tag{21}$$

$$S'(u,v) = I_{i,i-1}(s_i, s_{i-1})' B_{i,i-1}^{\mathrm{RH}}(u,v) + I_{i+1,i}(s_{i+1}, s_i)' B_{i+1,i}^{\mathrm{RH}}(u,v). \tag{22}$$

Consequently, we can prove Equations (18) and (19) by noticing that

$$B_{i,i-1}^{\mathrm{RH}}(u,v) + B_{i+1,i}^{\mathrm{RH}}(u,v) = 1. \tag{23}$$

6. The Generalized Bézier (GB) Patch

The Generalized Bézier patch is defined by a multi-sided control grid; the scheme has been introduced recently by the current authors.[10] It is a full generalization of quadrilateral Bézier patches, both in terms of its control structure and its behaviour along the boundaries.

The cross-derivatives along the boundaries are determined by the first two rows of control points. For a degree d GB patch, we define the number of *layers* (rows) as $l = \lceil d/2 \rceil$. For example, Figure 3 shows the control points of a five-sided quintic patch with 3 layers. It can be seen, that the control point structure associated with a given side is identical to that of a quadrilateral Bézier patch.

Coloring shows a classification of the control points: at the corners there are four *corner control points* (red), these

are associated with the i-th *and* $(i+1)$-th side. Between these, there are *ribbon control points* (green), these are associated exclusively with the i-th side. There are *interior control points* (yellow) in the middle, which can be placed automatically by a degree elevation algorithm. Finally, there is a single *center control point* (blue), that is responsible for the middle of the patch.

The behaviour of the GB patch at the boundaries is defined by the corresponding layers only; assume there is an edge shared by an adjacent quadrilateral or multi-sided patch having compatible rows of control points, then the connection will be smooth, as if ordinary quadrilaterals were connected.

The GB patch is defined over a regular polygonal domain in the (u,v) plane. The side and distance parameters s_i and h_i are defined by the barycentric scheme, as in the case of MP patches, see Section 5.1. The patch equation is

$$S_{\mathrm{GB}}(u,v) = \sum_{i=1}^{n} \sum_{j=0}^{d} \sum_{k=0}^{l-1} C_{j,k}^{d,i} \mu_{j,k}^{i} B_{j,k}^{d}(s_i,h_i) + C_0 B_0(u,v), \tag{24}$$

where n is the number of sides. The indexing scheme is side-based: $C_{j,k}^{d,i}$ refers to the j-th control point in the k-th row of the i-th side. Note that most control points have two indices, e.g. $C_{2,1}^{5,1} = C_{4,2}^{5,0}$.

The control points $C_{j,k}^{d,i}$ are multiplied by a biparametric Bernstein polynomial $B_{j,k}^{d}(s,h) = B_j^d(s) \cdot B_k^d(h)$ and a rational function $\mu_{j,k}^{i}$ (see below); the central control point C_0 is multiplied by the weight deficiency B_0, such that the sum of all weights becomes 1.

The scalar multipliers $\mu_{j,k}^{i}$ take on constant values (0, 0.5 or 1), except for those associated with the corner control points, see Figure 3. In this latter case, rational expressions of the distance parameters are used:

$$\alpha_i = \frac{h_{i-1}}{h_{i-1}+h_i}, \qquad \beta_i = \frac{h_{i+1}}{h_{i+1}+h_i}. \tag{25}$$

These weights are needed to ensure G^1 continuity, although the choice of 0.5 for $\mu_{j,k}^{i}$ (where $j=k$ or $j=d-k$) is quite arbitrary.

It has been proved in the original paper,[10] that GB patches interpolate the position and first cross-derivative of Bézier surfaces created by the first two rows of the related sides. The paper also presents a method to unite Bézier ribbons of various degrees into a single patch via degree reduction and elevation algorithms.

6.1. Controlling Blend Deficiency

In this section we will discuss how one can set the variation of the blending functions within the domain, and accordingly the central weight deficiency of GB patches. Reparameterizing the distance parameters provides an additional degree of freedom, by means of which it is possible to modify the interior shape properties in a favourable manner.

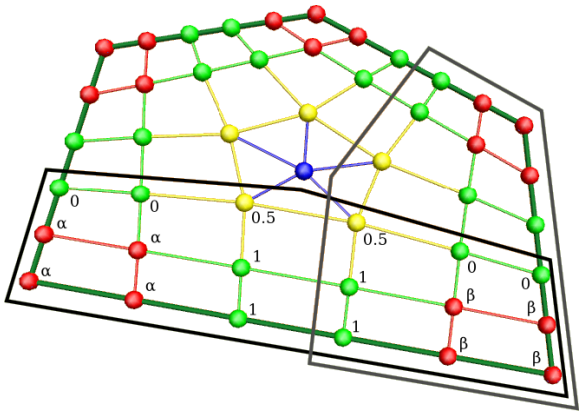

Figure 3: Rational weights of the GB patch. Black frames show the layers associated with two sides.

n	3	4	5	6	7	8
$d=3$	-0.11	0.00	0.12	0.22	0.31	0.38
$d=4$	-0.22	0.14	0.38	0.54	0.65	0.72
$d=5$	-0.43	0.00	0.29	0.47	0.59	0.68
$d=6$	-0.48	0.10	0.44	0.63	0.75	0.82
$d=7$	-0.61	0.00	0.37	0.59	0.72	0.80

Table 2: Blend deficiencies of the GB patch at the domain center as a function of the degree and the number of sides.

This reparameterization has been proposed earlier by Salvi et al.[8] We retain the basic properties of the original parameterization along the edges of the domain polygon, but modify the distribution of the h_i isoparameter lines by a biquadratic function in the interior. We can set the distance parameter at the domain center to an arbitrary x value by the following formula:

$$\hat{h} = h\left(1 + 4(1-s)s(1-h)h \cdot \frac{(x-h_c)}{(1-h_c)h_c^2}\right), \tag{26}$$

where $h_c = h(u_0,v_0) = (n-2)/n$. Default and reparameterized isolines are shown in Figure 4.

Table 2 shows the blend deficiencies at the domain center for various degrees and number of sides without reparameterization. We can observe that the default yields negative values for $n=3$, which would lead to a counter-intuitive (reverse direction) sense to the movement of the central control point. This can be avoided easily when reparameterization is applied. Another observation is that if we increase the number of sides and/or the degree, the central weight deficiency

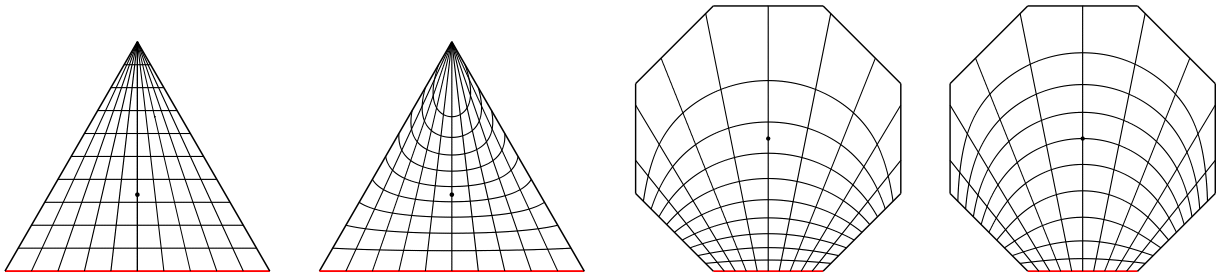

(a) $n = 3$, $d = 7$ (left: default, right: $\hat{h}(u_0, v_0) \approx 0.45$)

(b) $n = 8$, $d = 7$ (left: default, right: $\hat{h}(u_0, v_0) \approx 0.60$)

Figure 4: Reparameterization to ensure zero deficiency.

n	3	4	5	6	7	8
$d = 3$	0.39	0.50	0.57	0.61	0.65	0.67
$d = 4$	0.39	0.47	0.51	0.55	0.58	0.60
$d = 5$	0.44	0.50	0.54	0.58	0.60	0.62
$d = 6$	0.43	0.48	0.52	0.55	0.57	0.59
$d = 7$	0.45	0.50	0.54	0.56	0.58	0.60
$h(u_0, v_0)$	0.33	0.50	0.60	0.67	0.71	0.75

Table 3: Central distance parameter values for zero deficiency. The bottom row shows the default values.

also increases drastically, which may result in an excessive weight assigned to the center point; this is not desirable, as it may reduce the weight of the surrounding control points. Reparameterization helps to set the central weight as strong as requested, however, it should be noted that finding the optimal values is still subject of ongoing research.

It is also possible to compute x values that set the deficiency to zero (see Table 3). In this case the central control point has no effect at all. Experience shows, that zero settings create only moderate changes in the parameterization, and do not change surface quality significantly. Examples are shown in Figure 4.

7. Discussion

In the previous sections we have summarized the mathematical formulation of the CB, MP and GB patches.

(i) It was shown that CB patches are defined by arbitrary boundary curves and cross-derivatives, with a distance-based parameterization and high-degree rational blending functions. These patches have no weight deficiency, thus the only option for fullness control is to adjust the magnitude of the ribbons—see the constant w_i in Eq. (1).

(ii) MP patches also interpolate arbitrary boundary curves and cross-derivatives, but apply a more sophisticated barycentric distance parameterization with rational Hermite blending functions. These are low-degree rational polynomials, and their degree does not depend on the number of sides. The MP equation contains an extra term due to the weight deficiency of the RH blends, and this offers an additional tool to explicitly prescribe the middle point of the patch.

(iii) GB patches belong to another surface family, defined by a set of control points. In this case, the boundaries and cross-derivatives are defined by the first two rows of the multi-sided control grid. This representation is also based on the barycentric distance parameterization, but here control points are associated with Bernstein-like rational blending functions, thus providing high degree geometric freedom for manipulating the interior of the patch, when needed. It is also possible to elevate the degree of GB patches to gain additional control points.

It would be hard to demonstrate the editing capabilities of these patches, however, it is possible to compare how these patches could approximate various triangular meshes. Two examples will be analyzed.

7.1. Example 1—Synthetic Mesh

Our first example is a six-sided patch on a dense mesh of a sphere octant, see Figure 5. The boundaries run on the spherical surface, and the cross-derivatives are also set accordingly. With its default boundary ribbons, the CB patch yields a fairly rough approximation. When the ribbon multipliers are also optimized, a more accurate approximation is obtained, see related deviation maps in Figures (a) and (d), respectively. Dragging the midpoint of an MP patch onto the sphere improves the default deviation map, see Fig. (b). Here we can further optimize the ribbon magnitudes, as well, yielding a more accurate patch, see Fig. (e). In the last case, the boundaries and the cross-derivatives are represented as accurate approximations of the sphere, given in Bézier form. A default 5-degree GB patch is shown in Fig. (c), as a rough

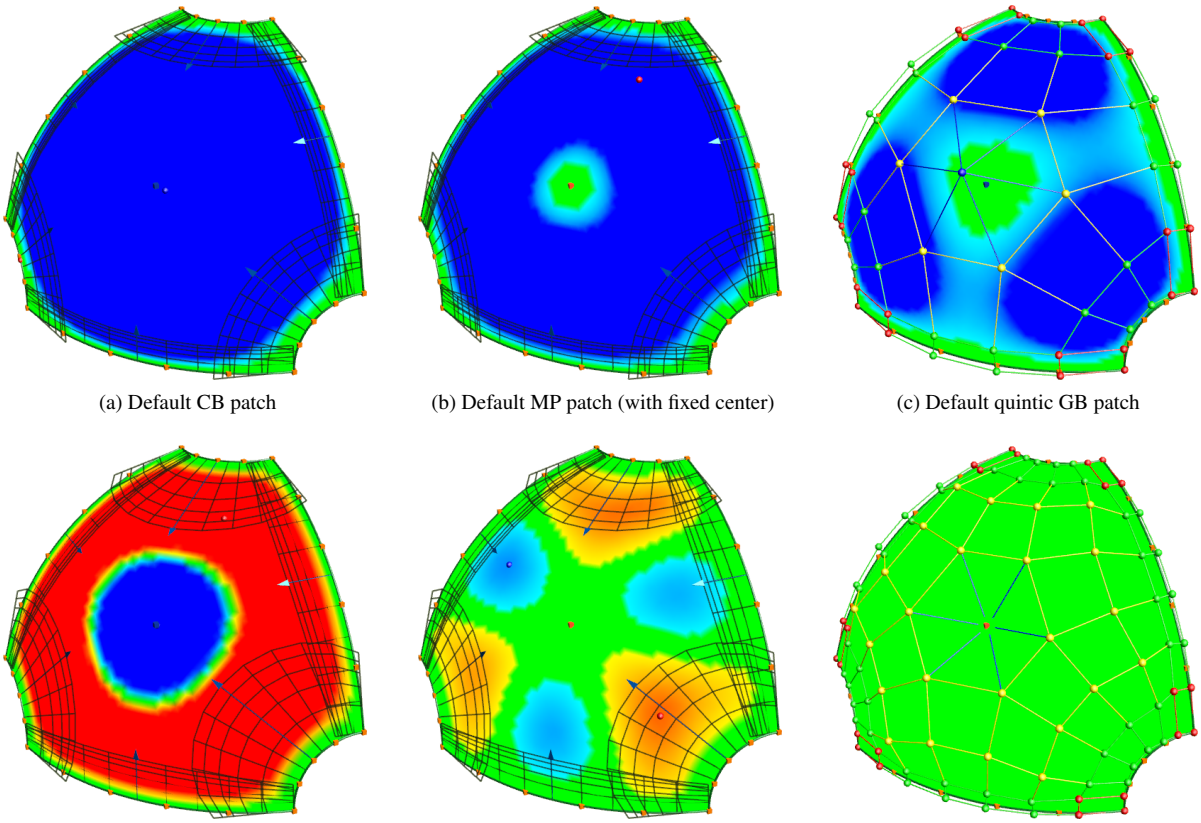

(a) Default CB patch (b) Default MP patch (with fixed center) (c) Default quintic GB patch

(d) Optimized CB patch (e) Optimized MP patch (with fixed center) (f) Optimized septic GB patch

Figure 5: Comparison on synthetic data: images show deviations from a dense sphere octant mesh with radius 100; green shows the range ± 0.05, red and blue have maximum intensity at ± 0.2. Red and blue markers show the places of maximum deviation.

	CB	MP	GB
Octant default	5.43%	0.46%	0.38%
Octant optimized	0.61%	0.09%	0.03%
Car default	6.68%	1.17%	1.06%
Car optimized	1.27%	1.11%	0.37%

Table 4: Numeric comparisons—all values are maximum deviations from the mesh, shown as (rounded) percentages of the bounding box axis.

approximation of the sphere. Elevating the degree, and optimizing the control points, including the interior control points (yellow) and the center control point (blue), leads to a very accurate patch that satisfies the preset tolerance criterion for the full patch. Table 4 shows the maximum deviations for all the above six cases.

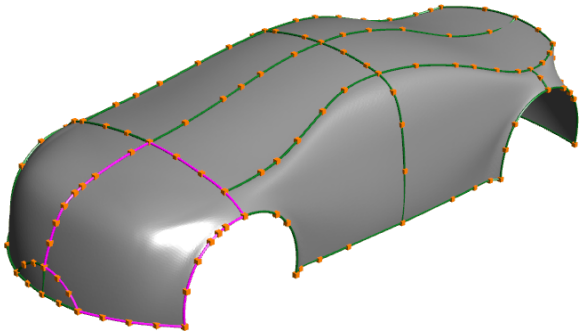

Figure 6: Mesh of a concept car and a network of feature curves. The curves defining the surface in Example 2 are highlighted.

7.2. Example 2—Concept Car

In the second example, we investigate how one can approximate the mesh of a large car model, see Figure 6. Only a

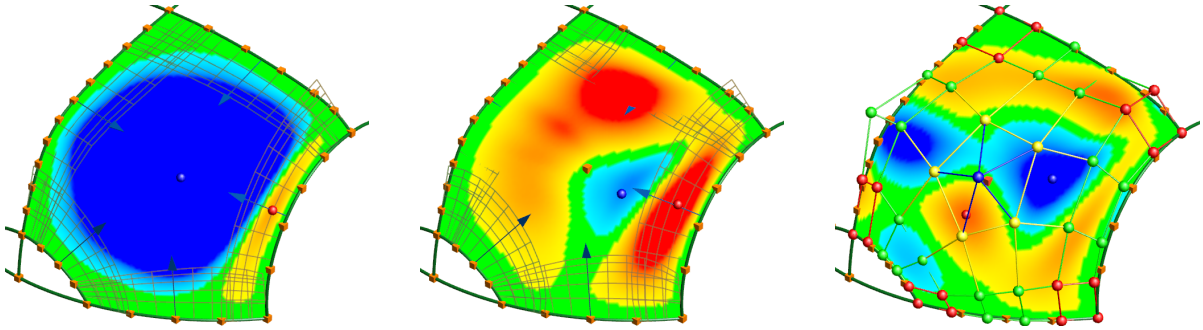

(a) Default CB patch (b) Default MP patch (with fixed center) (c) Default quintic GB patch

(d) Optimized CB patch (e) Optimized MP patch (with fixed center) (f) Optimized septic GB patch

Figure 7: Comparison on real data: images show deviations from a car body part with a bounding box axis of 1885mm; green shows the range $\pm$2mm, red and blue have maximum intensity at $\pm$12mm. Red and blue markers show the places of maximum deviation.

few feature curves have been drawn onto the mesh, bounding eight 5-sided, six 4-sided and two 3-sided patches. The main challenge is to achieve a good approximation of the underlying mesh despite the small number of surfaces. The cross-derivatives are calculated by estimated surface normals at the curve markers. We have picked a 5-sided patch for testing, that is strongly curved in both directions and also has an additional shape variation over the wheel.

Figure 7 shows the results of using different types of patches, with and without optimization, analogously to the previous example. We can see that the best approximation is achieved by the GB patch, as before. It is a relatively large error, but reasonable considering the sparse set of curves. A more accurate representation could be achieved by adding subdivision curves at the highly curved parts.

Conclusion and Future Work

We have investigated three multi-sided schemes with different degrees of freedom for adjusting the surface interior. These schemes differ with respect to the geometric entities available for shape adjustment. CB patches are derived from ribbon surfaces that have additional weights to set the magnitudes of the cross-derivatives, thus producing "stronger" or "weaker" fullness in the middle. MP patches offer an extra surface point to be set and interpolated, in addition to the ribbons and optimized magnitudes. GB patches are based on a multi-sided control grid, where the external rows of control points satisfy the boundary constraints, while the interior control points are generated by an automatic mechanism and can be used for further shape adjustment.

The underlying mathematical structure of these schemes are, of course, different. First of all, they differ in the parameterization of the polygonal domain, and the construction of blending functions that combine the controlling geometric entities. We have presented a new blending function to define the MP patch. A modification of the barycentric parameterization scheme has also been discussed, to adjust the weight deficiency of both the MP and GB patches.

We have compared these multi-sided schemes through their capabilities of approximating meshes, and numerically demonstrated the expected improvements in the case of MP and GB patches. MP patches seem to be a good choice for ribbon-based transfinite interpolation. GB patches, defined by Bézier-type boundaries, provide a high-degree of freedom for fullness control.

There are several open questions concerning the GB patch, such as the optimal setting of weight deficiency, algorithms for approximation and fairing, and extending the scheme to B-spline boundary curves, as well.

Acknowledgements

This work was partially supported by a grant from the Hungarian Scientific Research Fund (No. 101845), the Suzuki Foundation, and the Budapest University of Technology and Economics. The pictures were generated by the Sketches system (ShapEx Ltd, Budapest); the authors appreciate the help of György Karikó with the implementation.

References

1. Alan A. Ball and Jinjin Zheng. Degree elevation for *n*-sided surfaces. *Computer Aided Geometric Design*, 18(2):135–147, 2001.
2. John A. Gregory. *n*-sided surface patches. In *Mathematics of Surfaces I*, pages 217–232. Oxford University Press, 1986.
3. Kai Hormann and Michael S. Floater. Mean value coordinates for arbitrary planar polygons. *Transactions on Graphics*, 25(4):1424–1441, 2006.
4. Mamoru Hosaka and Fumihiko Kimura. Non-four-sided patch expressions with control points. *Computer Aided Geometric Design*, 1(1):75–86, 1984.
5. Kiyokata Kato. Generation of *n*-sided surface patches with holes. *Computer-Aided Design*, 23(10):676–683, 1991.
6. Charles T. Loop and Tony D. DeRose. A multisided generalization of Bézier surfaces. *Transactions on Graphics*, 8:204–234, 1989.
7. Péter Salvi and Tamás Várady. G^2 surface interpolation over general topology curve networks. *Computer Graphics Forum*, 33(7):151–160, 2014.
8. Péter Salvi, Tamás Várady, and Alyn Rockwood. Ribbon-based transfinite surfaces. *Computer Aided Geometric Design*, 31(9):613–630, 2014.
9. Tamás Várady, Alyn Rockwood, and Péter Salvi. Transfinite surface interpolation over irregular *n*-sided domains. *Computer Aided Design*, 43(11):1330–1340, 2011.
10. Tamás Várady and Péter Salvi. A multi-sided Bézier patch with a simple control structure. *Computer Graphics Forum*, 35(2), 2016 (accepted).
11. Tamás Várady, Péter Salvi, and Alyn Rockwood. Transfinite surface interpolation with interior control. *Graphical Models*, 74(6):311–320, 2012.
12. Jinjin Zheng and Alan A. Ball. Control point surfaces over non-four-sided areas. *Computer Aided Geometric Design*, 14(9):807–821, 1997.